Original
ISSN 2413-0516

Targeting Heat Shock Proteins for Enhanced Apoptosis in Hyperthermic Breast Cancer Therapy Using Nanoquercetin and Nanocobalt Ferrite

Alaa Sameer Neamah[1], Raziyeh Ghorbani[2], Mohammad Mahdi Ahadian[3], Simzar Hosseinzadeh[2,4*], Bahram Kazemi[1*]

[1]Department of Medical Biotechnology, School of Advanced Technologies in Medicine, Shahid Beheshti University of Medical Sciences, Tehran, Iran.
[2]Tissue Engineering and Applied Cell Sciences Department, School of Advanced Technologies in Medicine, Shahid Beheshti University of Medical Sciences, Tehran, Iran.
[3]Center for Nanoscience & Nanotechnology, Institute for Convergence Science and Technology (ICST), Sharif University of Technology, Tehran, Iran.
[4]Medical Nanotechnology and Tissue Engineering Research Center, Shahid Beheshti University of Medical Sciences, Tehran, Iran.
*Correspondence to: Dr. Simzar Hosseinzadeh (E mail: s.hosseinzadeh@sbmu.ac.ir), Bahram Kazemi (E mail: bahram_14@yahoo.com)
(Submitted: 09 November 2024 – Revised version received: 03 December 2024 – Accepted: 25 December 2024 – Published online: 26 February 2025)

Abstract

Objectives: The expression of heat shock proteins (hsps) in cells is dependent on cell stress and the high temperature of hyperthermia elevates them. Therefore, consideration of an attenuator of this pathway is needed.

Methods: After preparation and characterization of both nanoquercetin and magnetic nanoparticles, MCF7 cell line treated to determine the IC50 of both nanoparticles using MTT assay. The percentage of radical levels in all groups was investigated using DPPH technique. Also, Real-Time PCR was utilized to reveal the regulation of hsps and apoptotic genes.

Results: The diameter of the nanocobalt ferrite was 8.08 ± 2.5 nm indicating a soft-ferromagnetic property due to its zero coercivity. Also, the nanoquercetin exhibited a size of 42.42 ± 13.26 nm after encapsulation by chitosan. FTIR spectroscopy presented specific bands such as 1640, 1560 and 1380 cm^{-1} for amide I, II and III and 1600 and 1400 cm^{-1} for C=C stretching in aromatic rings, respectively for both chitosan and quercetin. The cell viability by MTT assay were 10 and 0.6 mg/ml for cobalt ferrite and quercetin as IC50 concentrations. After applying hyperthermia with a frequency of 350 kHz and a treatment duration of 10 min, the highest degree of radical inhibition was observed in the combination condition under hyperthermia, with a value of 21.03 ± 0.2 %. Moreover, the Bax/Bcl2 ratio of 6.66 in the composite group suggests an apoptotic fate for the cells. The composite and nanoquercetin treatments showed the highest fold changes of 1.4 and 43 for caspase 3. In contrast, caspase 8 exhibited values of 25 and 0.25 for these groups, respectively.

Conclusions: The treatment of cells with a blocker of hsps such as quercetin increases the yield of hyperthermia. However, more investigations are needed, particularly in animal models to introduce this nanoformulation for clinical trials.

Graphical Abstract

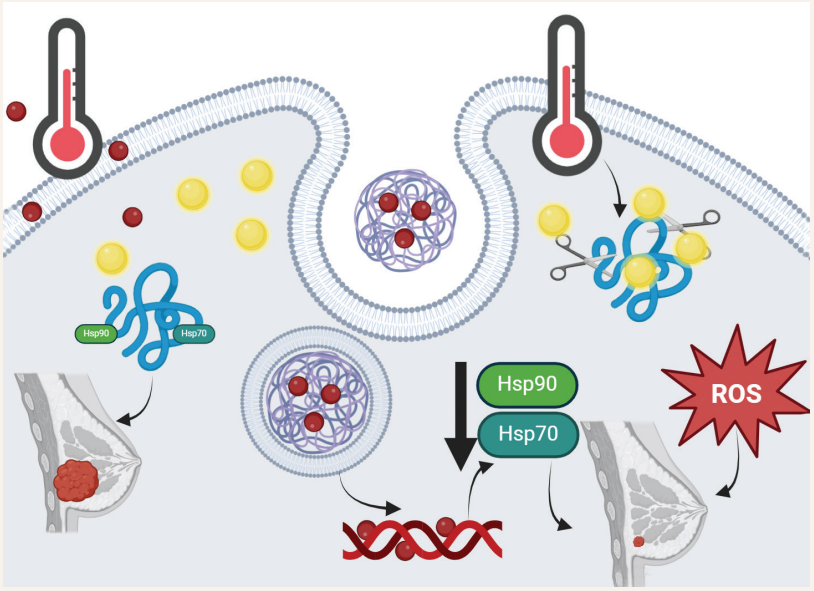

The treatment of cancer cells by nanoquercetin increases the bioavailability of this hydrophobic compound. The higher concentration results in reduced expression of heat shock proteins such (HSP) as HSP70 and HSP90. As a consequence, cellular proteins are less protected against the elevated temperatures associated with hyperthermia and ultimately leading to cell death through reactive oxygen species (ROS) production.

Keywords: Breast cancer, hyperthermia, nanoquercetin, cobalt ferrite, heat shock proteins

Introduction

Breast cancer ranks among the most frequently diagnosed cancers globally. Treatment options for this cancer are radiotherapy and chemotherapy, but these methods often come with significant side effects on healthy cells and also, low efficacy.[1] In the recent years, researches have been increasingly focused on discovering new drugs for breast cancer treatment. Among the methods, some plant-derived bioactive compounds can act as pro-oxidants and generate reactive oxygen species (ROS) within cancer cells.[2] This oxidative stress can disrupt signaling pathways, damage DNA, and influence on the progression of various cancers, including colon, prostate, lung, ovary, and breast cancers. Superoxide dismutase (SOD) and catalase (CAT) are key enzymatic antioxidants that help neutralize ROS in cancer cells.[3] Colloidal iron oxide and iron oxide-based core-shell nanostructures are particularly popular due to their size-dependent magnetic properties, making them ideal candidates for biomedical applications and *in vivo* experiments.[4] For cancer therapy, a lot of researches focuses on iron oxide-based nanoparticles with superior magnetic properties for effective destruction of cancer cells via hyperthermia.[5] One of iron oxide derivatives is cobalt ferrite ($CoFe_2O_4$) as a function of its high anisotropy, can enhance the efficiency of hyperthermia to apply cell apoptosis.[6] Hyperthermia, a widely recognized therapeutic method, involves exposing tumor tissues to high temperatures to damage them or enhance their sensitivity to radiation and certain anticancer drugs.[7] This method in compared to other techniques such as laser, ionizing radiation, and microwaves, indicate minimum damages to surrounding healthy tissues due to targeting the temperature by using magnetic nanoparticles.[8] However, at temperatures higher than physiological levels, this method increases the expression of heat shock proteins (hsps).[9] Hsps belongs a diverse group of molecular chaperones classified by their molecular weights to HSP27, HSP40, HSP60, HSP70, and HSP90. These proteins make protein folding, maturation, and degradation in response to different stress conditions such as heat shock and hypoxia.[10] By applying hyperthermia, the expression of these proteins is elevated and thus, attenuates the efficacy of this method. Quercetin is well-known as a potent agent that can inhibit hsps and facilitate the impact of hyperthermia.[11] This compound as a potent flavonoid found in foods such as onions, red grapes, lettuce, tomatoes, olive oil, tea, coffee, bracken fern, and citrus fruits, has been shown to have toxic effects on various cancer cells.[12] Despite its potential, the therapeutic of this factor has been hindered by its poor solubility and low bioavailability.[13] To enhance the bioavailability of anticancer agents, several drug delivery systems have been explored, including polymeric nanoparticles, solid lipid nanoparticles (SLNs), liposomes, and micelles.[14] Encapsulating a drug in nanoparticles can enhance its stability, extends its circulation time, and increases its accumulation in tumors, leading to improved therapeutic results.[15] This chemical factor reduces tumor multidrug resistance via inhibiting P-glycoprotein, downregulation of multidrug resistance-related proteins and by reducing intracellular Glutathione levels.[16] Beside passive targeting of drug delivery to tumor tissue, active targeting may be achievable by the combination of a chemical nanodrug and magnetic nanoparticles with high saturation magnetization.[17] Regarding to this, the combination of magnetic nanostructures and nanoquercetin may promote the outcome of hyperthermia. In a study, quercetin was nanoformulated as liposomes and in synergistic manner with Fe_3O_4 nanoparticles recruited to hyperthermia against MG-63 osteosarcoma cells. The results confirmed a lower cell viability in *in vitro* model.[18] Another investigation used iron oxide nanoparticles which were cross-linked to nanoquercetin under the culture of MCF7 cells. This study was performed in the absence of hyperthermia and the results approved the more toxicity of the composite particle against pure quercetin.[19] A group loaded quercetin and cobalt ferrite on liposomes and treated MCF7 cells by hyperthermia. They found 35% and 55% of early and late apoptosis, respectively. This study was limited to cell culture and proliferation.[20] Another report was discussed about the toxicity of graphene oxide loaded by an iron oxide derivative and quercetin against HEK 293-T and MCF7 cells. The assays unveiled in the presence of UV light, the destruction of the cells was increased.[21] Also, a similar study fabricated nanoparticles containing iron oxide/folic acid/quercetin for therapeutic approaches of brain cancer. This examination was done without any hyperthermia conditions and only, confirmed that the nanoparticles could enter the cells and applied toxicity.[22] The chitosan nanoparticles loaded by quercetin and iron oxide revealed apoptotic cell death against H522 cell line and also, neutralizing free radicals were occurred.[23] Moreover, cobalt ferrite was loaded on the graphene oxide sheets and in the presence of hyperthermia and bulk quercetin. The observations approved that the combination strategy made lower expression of hsps in MCF7 cells and also, higher toxicity.[24] For first time in the present study, the impact of quercetin-chitosan nanoparticles in the simultaneous model with cobalt ferrite nanostructures was evaluated on MCF7 cells. Also, beside hyperthermia, the regulation of apoptotic genes and hsps was surveyed.

Materials and Methods

Preparation of $CoFe_2O_4$ Nanoparticles

The nanoparticle was synthesized by adding 0.47 g of cobalt chloride to 10 ml of distilled water. Then, 1.6 g of nitrate iron (Sigma) and 0.06 g of PVP (Sigma) were weighted and added. The final mixture was stirred for 4 hrs to get a homogenous solution. The pH was changed to 11–14 after this incubation by using ammonium solution (25%, Sigma). The corresponding solution was poured to a metal container and its lid was sealed and stored in an oven at 180°C for 3 hrs. The product was cooled and poured to a beaker and let to sediment. Then, the material was washed with distilled water for several times and its supernatant was thrown away. For the cell culture investigations, the nanoparticle was mixed with phosphate bovine sulfate (PBS, Gibco) and ultra-sonicated for 15 min and then, added to the cells at predetermined concentrations.

Transmission Electron Microscope (TEM)

The magnetic nanoparticles were investigated by using a Zeiss-EM10C TEM (Oberkochen, Germany). The nanoparticles at the concentration of 0.005 gr/ml were suspended in PBS and poured on a carbon-coated copper grid. The accelerating voltage was 80 kV and the sample was studied by TEM apparatus.

Vibrational Sample Magnetometer (VSM)

The magnetic behavior of the cobalt ferrite nanoparticles was investigated by using a VSM apparatus (VSM-7300, Meghnatis

Daghigh Kavir Co., Kashan, Iran). The maximum applied field was 15 kOe and the temperature was almost room condition. The final curves were evaluated to judge the magnetic property of the corresponding nanoparticle.

Preparation of Quercetin Nanoparticles

Quercetin (Sigma) nanoparticles were developed by using quercetin purchased from sigma. For this process, the quercetin was dissolved in absolute ethanol (16% w/v, Merck). Then, chitosan (low molecular weight, Sigma) at the concentration of 0.2% w/v was poured to acetic acid (Merck). After chitosan dissolving, the pH value was changed to 5.5 by adding NaOH (Sigma) solution. The chitosan and quercetin solutions were mixed each other at the ratio of 5:1. On the other hand, trisodium phosphate (TPP, Sigma) solution at the concentration of 1% w/v, was gradually added to the blend solution of chitosan and quercetin. This step must be done under magnetic stirring and room temperature. The volume of the solution was increased to 50 ml by adding distilled water. Then, the sample was filtered (0.2 μm) and centrifuged at 13000 rpm/min for 15 min. The supernatant was discarded and water added to wash out the non-trapped quercetin. After all, acetic acid was added to remove the free chitosan by centrifuging the sediment again at same conditions. Finally, the precipitate sample containing chitosan-quercetin nanoparticles, was collected.

Scanning Electron Microscope (SEM)

The shape of the quercetin nanoparticles was illustrated by SEM (S-4500; Hitachi, Tokyo, Japan). The gold was coated by a sputtering (Quorum Technologies-Emitech-SC7620 model) and then, the sample was examined by SEM.

Dynamic Light Scattering (DLS)

The homogeneity of the quercetin nanoparticles was studied by dynamic light scattering (DLS, Malvern Instruments, Worcestershire, UK) at room temperature. For this method, the nanoparticle sample was diluted by adding distilled water and then, load on the apparatus. The parameters including particle dispersion index (PDI), average particle size and its related curve were reported.

Fourier Transform Infrared (FTIR) Spectroscopy

The chemical groups of quercetin and chitosan were detected by using a Fourier transform infrared spectroscopy (FTIR, Spectrum RX I, USA). For this assessment, the sample was freeze dried for 24 hrs and then, the assay was done. The range of wavelengths was between 400–4000 nm and the scan rate was 2 nm.

Cell Culture and MTT Assessment

MCF7 cells were bought from Pasteur Institute of Iran and cultured under ethical number of IR.SBMU.RETECH.REC.1402.184 from shahid beheshti university of medical sciences, Tehran, Iran. The cells cultured in Dulbecco's Modified Eagle's Medium (DMEM, Gibco) supplemented with 10% fetal bovine serum (FBS, Gibco) and incubated at 37°C in a 5% CO2 humidified atmosphere. After 24 hrs, the cells were seeded into 96-well plates at a density of 8×10^3 per a cell well. The experimental groups were treated with magnetic nanoparticles at concentrations of 0.5, 2, 5, 10, 20 and 30 mg/ml and 0.1, 0.3, 0.6, 1.2 mg/ml for the quercetin. The tissue culture polystyrene control (TCPS) group was considered as the control group which was not treated. The 3-[4,5-dimethylthiazol-2-yl]-2,5-diphenyl tetrazolium bromide (MTT, Sigma) assay was done after 24, 48, and 72 hrs to determine the IC50 values of both nanoparticle types. For this assay, the cells were washed with PBS and the MTT solution (0.1 mg/ml in DMEM without FBS) was added to each well and incubated for 3.5 hrs. The formazan crystals were collected by using dimethyl sulfoxide (DMSO, Merck), and the absorbance values were measured at 570 nm. Once the IC50 concentration was determined, the hyperthermia treatments were conducted. The power (1000 W), frequency (350 kHz) and treatment time (10 min) was done accordance with the before experiment which was published before.[25] The cell viability (%) values were calculated by the following formula:

$$\text{Cell viability (\%)} = \text{OD of experimental group/OD of TCPS}$$

Here, OD is abbreviated of optical density and the experimental and TCPS groups were the treated and non-treated groups, respectively.

DPPH Assay

The value of free radicals was measured by 1,1-diphenyl-2-picrylhydrazyl (DPPH, Sigma) assay. For this assay, DPPH solution at the concentration of 1 mM in methanol (Merck) was added to the cells. Then, the groups including treated and non-treated, incubated by DPPH solution in darkness for 30 min. Their absorbance values were read at 520 nm and their inhibition values (%) were calculated by the below formula:

$$\text{Radical inhibition (\%)} = (\text{OD of blank} - \text{OD of experimental group})/\text{OD of blank} \times 100$$

Here, OD is abbreviated of optical density and the experimental and blank groups were the treated samples and pure DPPH solution, respectively.

Real-Time PCR

Total RNA was extracted from MCF7 cell line using RNXplus reagent (Gibco) according to the manufacturer's instructions. RNA concentration and its purity were determined by using a nanodrop spectrophotometer (Thermo Fisher Scientific, USA). Complementary DNA (cDNA) was synthesized from RNA using AddBio cDNA synthesis kit with random hexamer primers (Gibco). Real-time PCR was performed using with SYBR Green (Biorad). The sequence of the primers which were employed in this assay, is reported in Table 1. The thermal cycling conditions were as follows: initial denaturation at 95°C for 10 min, followed by 40 cycles of denaturation at 95°C for 15 s and annealing/extension at 60°C for 1 min. The expression of mRNA was normalized to GAPDH as a house keeping gene by ΔΔCt method. The results were reported as fold changes which were obtained against the TCPS group, relatively.

Statistical Analysis

All observations were statistically evaluated by sigma-plot software and the relation between 2 groups was checked by student's t-test. The assays were repeated at least for 3 times except FTIR and TEM. When the *P*-value was lower than 0.05, the comparison was significant and the equal or higher values were considered as insignificant. The all quantitative values were shown as mean ± standard error.

Table 1. **The primer sequences which were used for Real-Time PCR assessment**

No.	Name of gene	Primer sequence
1	H-HSP90-R	TCTCTTTATCTTCCGCC
2	H-HSP90-F	AATCCCTGAATATCTGAACT
3	HSP70-F	GAGTCCTACGCCTTCAA
4	HSP70-R	GCACCTTCTTCTTGTCC
5	HPRT1-F	CCTGGCGTCGTGATTAGTG
6	HPRT1-R	TCAGTCCTGTCCATAATTAGTCC
7	H-BAX-F	CAAACTGGTGCTCAAGGC
8	H-BAX-R	CACAAAGATGGTCACGGTC
9	H-BCL2-F	GATAACGGAGGCTCCCATG
10	H-BCL2-R	CAGGAGAAATCAAACAGAGGC
11	HSP70-F	GCTATTATGGCAGATAGACAGAG
12	HSP70-R	TGTTACGATCTTCACTCAC

Results

TEM and VSM examinations of cobalt ferrite nanoparticles

The magnetic nanoparticles were investigated by TEM and shown in Figure 1. The size of the particles is 8.08 ± 2.5 nm. Due to the low standard deviation value, it could be claimed that the size of the particles was uniform. Accordance with other reports, this particle diameter which is lower than 20 nm, may shows superparamagnetic behavior.[26,27] In contrast, other researches confirmed that the critical size of this material for superparamagnetic property with zero coercivity and remanence, was 7 nm. The larger particle radius leads into higher magnetization and a small coercivity. This manner is useful for the applications of magnetic particles in hyperthermia.[28] The resulting coercivity is happened as a coupling between the spins of cobalt and iron.[29] Also, the VSM analysis reveals several key magnetic properties of the cobalt ferrite nanoparticle in Figure 2. The hysteresis loop displayed in the graph, is representing typical ferromagnetic behavior due to its distinctive sigmoid-shape.[30] The saturation magnetization (Ms) is approximately 68 emu/g, indicating the maximum magnetization achieved under a high applied magnetic field.[31] The remanent magnetization (R_m) is around 5 emu/g, showing a small residual magnetization when the external magnetic field is almost reduced to zero. The coercive field (Hc) which represents the required magnetic field to bring the magnetization to zero, is almost 0 Oe, highlighting the material's low resistance to becoming demagnetized. The low coercivity suggests that the sample is a soft-ferromagnetic material, meaning it loses magnetization upon the magnetic field turns off.[32] These characteristics are crucial for applications such as hyperthermia particularly intratumoural target.[33]

SEM, DLS and FTIR Examinations of Quercetin-Chitosan Nanoparticles

The as-synthesized nanoquercetin particles were evaluated by SEM and reported in Figure 3. The size of the particles 42.42 ± 13.26 nm representing high homogeneity between the particle diameter. Accordance with other investigations, the sizes between 50 to 200 nm can easily transfer via vascular pores to reach tumor cells.[34] This size is lower than the particles which were fabricated by lipid nanoparticles to treat human breast cancer as 85.5 nm. The corresponding diameter made higher cytotoxic effect due to its higher uptake in compared to free quercetin.[35] Another study with a diameter of 30–40 nm, quercetin nanoparticles reduced cancer growth in mice bearing tumor.[36] This particle diameter is almost near to the result of an investigation preparing quercetin nanoparticle using chitosan (50 ± 3 nm).[37]

The FTIR spectrum of the synthesized nanoquercetin by using chitosan reveals several significant absorption peaks, which provide insights into its molecular structure (Figure 4a).

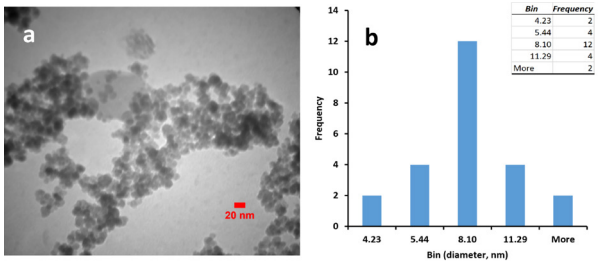

Fig. 1 **Particle diameter and its distribution by TEM examination (a) and diameter histogram (b) of cobalt ferrite nanoparticles.**

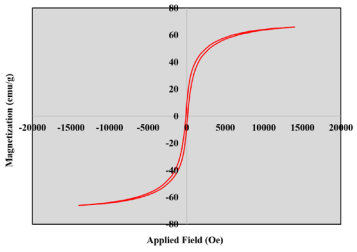

Fig. 2 **Magnetic property of cobalt ferrite nanoparticles by VSM survey.**

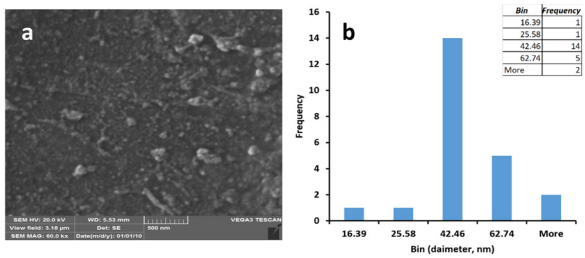

Fig. 3 **Particle diameter and its distribution by SEM examination (a) and diameter histogram (b) of quercetin nanoparticles.**

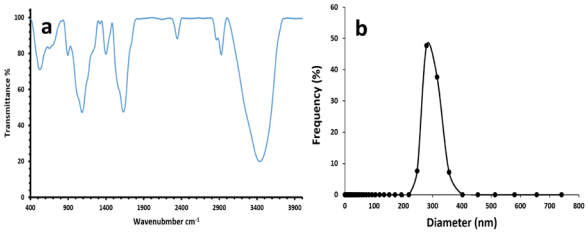

Fig. 4 **Chemical groups of chitosan and quercetin by FTIR spectroscopy (a) and nanoquercetin hydrodynamic diameter by DLS assay (b) of quercetin nanoparticles.**

The broad and intense absorption band around 3400 cm^{-1} indicates the presence of O-H stretching vibrations, suggesting the presence of hydroxyl groups or water molecules.[38] The peaks observed near 2900 cm^{-1} can be attributed to C-H stretching vibrations, typical for aliphatic hydrocarbons.[39] A strong peak around 1700 cm^{-1} corresponds to the C=O stretching vibration, indicating carbonyl groups, such as those found in ketones, aldehydes, or carboxylic acid.[40] The absorption bands around 1600 and 1400 cm^{-1} are likely due to C=C stretching in aromatic rings or other double-bonded systems such as quercetin.[41] Also, the peaks of 1640, 1560 and 1380 cm^{-1} are originated from amide I, II and III, respectively.[42] Additionally, the peaks between 1000 and 1300 cm^{-1} can be attributed to C-O stretching vibrations of the compounds such as alcohols, ethers, or esters.[43] The presence of the multiple peaks in the fingerprint region (below 1500 cm^{-1}) provides further confirmations of the complex molecular structure of the compound. These observations suggest that the synthesized particle contains functional groups such as hydroxyl, carbonyl, and possibly aromatic systems.

DLS of the synthesized nanoquercetin reveals a sharp and narrow size distribution, as depicted in Figure 4b. The majority of the particles almost 47%, exhibit a hydrodynamic diameter around 279.04 nm with the PDI of 0.22. This low value confirms a highly uniform distribution of nanoquercetin. Accordance with other reports, a PDI value below 0.3, typically indicates a monodisperse system,[44] suggesting that the synthesis process yielded particles with a consistent size. The narrow size distribution and low PDI are advantageous for the applications such as drug delivery, where a smaller diameter can elevate the rate of the release profile and also, cell uptake.[45] Other reports approved that a particle diameter lower than 200 nm are good candidate for drug delivery to tumors.[46] In contrast, the particles with a diameter larger than 100 nm, are lower trapped by reticuloendothelial system (RES) containing the cells derived from monocytes.[47] Therefore, their shelf-life in blood could be longer that is advantageous to higher clearance by the tissue. Also, other literatures suggested that any sizes between 1–1000 nm could trigger delivery of the drug to cancer cells.[48] As a whole, it could be concluded that the size near to 300 nm, increases quercetin delivery better than non-capsulated one. Also, this size would have a minimum immune system response.

IC50 Concentrations by MTT Assay

MTT method was employed to detect IC50 values of both nanoparticle types including nanoquercetin and cobalt ferrite (Figure 5). A toxic effect was revealed a dose-dependent manner upon treatment with the nanoparticles. For cobalt ferrite, at the highest concentration of 30 mg/ml, the cell viability reduced to 23.56 ± 0.4 %. There is another important data by considering the treatment time. Regarding to this, the particle effect on cell apoptosis, had been remained during time and the cells were not able to compensate cell death by proliferation. In contrast, the lowest value of this nanoparticle (0.5 mg/ml), showed the maximum cell viability (93.95 ± 12 %), although the cells started to proliferate after 48 and 72 hrs. This behavior was obeyed with the concentrations of 2 and 5 mg/ml. However, the killing effect of this nanoparticle was triggered at the higher concentrations. Therefore, the treatment group of 10 mg/ml could be introduced as IC50 of this nanoparticle with the cell viability of 46.11 ± 4 %. A same event was repeated with nanoquercetine at its higher concentrations. For this particle, there was no toxic effect when the value was 0.5 mg/ml and the cell viability was almost 100%. While, the cells lost their mitotic activity after 24 hrs and therefore, the apoptotic effect was preserved. By increasing the concentration, the cell viability was reduced significantly. In this manner, the concentration of 0.6 mg/ml caused stronger cell death which postponed cell proliferation over time with the cell viability of 47.83 ± 2 %. At the higher value of this nanoparticle, it seems the cell viability was not changed. Thus, the noted concentration was selected as IC50 of nanoquercetin.

Radical Development by DPPH Assay

The results of the DPPH assay presented the antioxidant activity of various samples in Figure 6. The bulk sample shows a radical inhibition of 6.94 ± 1.2 % with significant relations compared to both treated and non-treated groups by hyperthermia. This manner depicts a higher level of radicals in the presence of the cells and hyperthermia.[24] The NQ sample has a value of 8.81 ± 0.9 %, which is higher than the value of the blank group as a function of the scavenging activity of quercetin radicals.[49] The value is decreased to 5.61 ± 0.2 % in the group containing the magnetic nanoparticles. Also, it seems that the sample of cobalt ferrite was without any radicals. In contrast, after mixing nanoquercetin and cobalt ferrite with each other the value was increased to 9.30 ± 0.6 %, although with insignificant value in compared to the NQ sample. The sample with only MCF7 cells indicated 5.65 ± 0.1 % which is almost same to the group containing only magnetic nanoparticles. The values of the radical inhibitions with the hyperthermia treated groups illustrated a considerable high value in compared to the non-treated types. This result clearly confirms the potential effect of hyperthermia regarding to its effective role on radical synthesis.[50] Among these groups, a higher radical

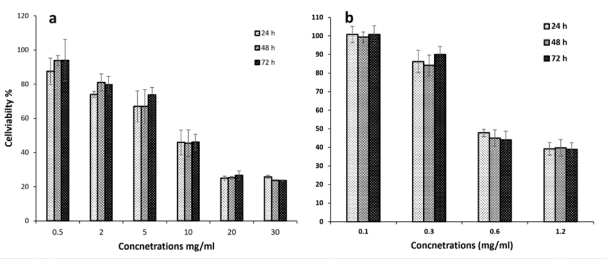

Fig. 5 **Cell viability (%) by MTT assessment to find out IC50 of cobalt ferrite (a) and quercetin nanoparticles (b) in a gradient concentration.**

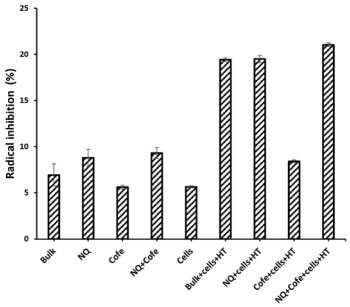

Fig. 6 **Radical inhibition (%) by DPPH assessment of the groups with and without hyperthermia, cells and nanoparticles.**

quenching was indicated in the presence of nanoquercetin. However, the value of bulk (19.42 ± 0.2%) and nanoscale (19.5 ± 0.4%) of this compound did not show significant difference. The result could be related to the controlled release of this material against explosive delivery of the bulk one. A cooperative manner was established when both nanoparticles were blended each other and the value was 21.03 ± 0.2 %. The corresponding data is in agreement with the apoptotic effect of the cells by hyperthermia which were treated by both nanoparticle types.

Gene Expression by Real-Time PCR

To investigate the effect of nanoquercetin and cobalt ferrite in the presence and absence of hyperthermia on cellular apoptosis. The expression of Bcl2, Bax, caspase 3, Caspase 8, hsp70 and hsp90 genes. Regarding Bax as a marker of cell apoptosis[51] and Bcl2 as a apoptosis blocker[52] in Figure 7, all groups indicated a lower expression value significantly. Even, this reduction was further due to the presence of both nanoparticles and hyperthermia treatment. The comparison among the Bax expression, the value was low in all experimental groups calibrated against TCPS. Again, the lowest value of Bcl2 was belonged to the combination group that is significantly distinguished in compared to other groups. Caspase genes including 3 and 8, their higher expressions lead into more cell apoptosis.[53] All groups except the combination and magnetic nanoparticle types, showed a fluctuated expression values. However, the expression of caspase 8 as an earlier gene had higher magnitudes with all groups except the bulk and combination in the absence of hyperthermia. This observation depicted a positive effect of hyperthermia on cell apoptosis. There are 2 groups with highest degrees of caspase 8 including the combination group and nanoquercetin without hyperthermia. However, the result confirmed more expression of caspase 3 in contrast to the nanoquercetin group. The hsps (70 and 90) as vital genes against higher temperatures,[54] increased with the groups without hyperthermia in contrary to the hyperthermia treated samples. It is obvious in Figure 8, the effect of NQ is stronger than the blocking impact of the free quercetin on the hsps. While, the treated group with the combination of both nanoparticles (NQ+cofe) depicted higher values in compared to the treated group with nanoquercetin (NQ). This observation confirmed the presence of the magnetic nanoparticles triggered the expression of the hsps and the NQ was not capable. In this manner, in the absence of hyperthermia, the negative effect of nanoquercetin on the expression of the hsps, was reduced significantly. In contrast, after hyperthermia process, the levels of both hsps were reduced. In other words, by comparing the value of the NQ and free quercetin in either hyperthermia or not, it could be concluded the nanoparticles indicated a stronger blocking impact on the expression of hsps when the cells were treated by hyperthermia. It is clear the nanoparticles can transfer easily from cellular membrane and also, at a high temperature, the chitosan capsule is degraded. Subsequently, the more quercetin is available to cells in compared to its bulk group. Regarding this, in the group with only NQ, the expression of the corresponding genes is high representing low blocking activities. But in the NQ+HT, the negative effect of quercetin was happened and subsequently, the expression was reduced.

Discussion

Breast cancer is the second leading cause of cancer-related death among women. In spite of recent advancements which have been made in the treatment of this disease, the incidence and mortality rates remain high. Current studies are shifting towards the use of combinatorial medicine, employing both physical and biochemical methods simultaneously to limit the disease progression. One of the most important strategies, is hyperthermia, especially in the presence of magnetic nanoparticles. Iron oxide nanoparticles such as cobalt ferrite ($CoFe_2O_4$) is an attractive one due to its high efficacy on hyperthermia as a stimulus of stronger apoptosis.[55] However, at temperatures higher than physiological levels, it raises the expression of hsps. The increase of these proteins represents a cellular response to unfavorable environmental conditions such as high temperatures. Therefore, there is an urgent need to inhibit the synthesis of these proteins. Quercetin is a flavonoid that can down-regulate them and thus, it leads the cancer cells into apoptosis.[56] Moreover, this compound has been introduced as a strong inhibitor of the proliferation of cancer cells[57] and also, establishing cell apoptosis via inhibiting of p38MAPK–Hsp27 pathway belonged to drug resistance of cancer cells.[58] On the other hand, a notable problem is associated to its hydrophobicity and disability to enter cancer cells.[59] An attractive method has been suggested to solve this issue by formulating it as nanoparticles by using emulsifying agents[60] or polymers.[61] In present study, the combination of magnetic nanoparticles and chemical factor (nanoquercetin) beside

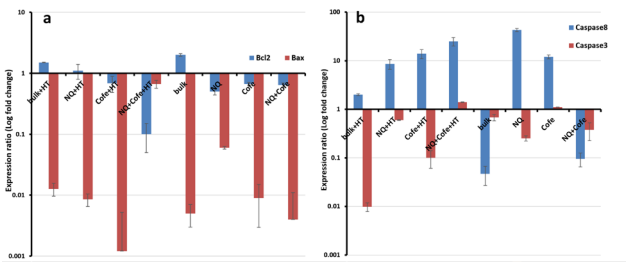

Fig. 7 **Relative fold change values by Real-Time PCR for (a) bcl2 and bax and (b) caspase 3 and 8 genes of the groups with and without hyperthermia, cells and nanoparticles.**

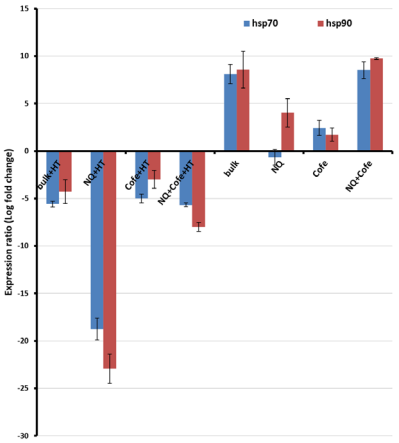

Fig. 8 **Relative fold change values by Real-Time PCR for hsp70 and 90 of the groups with and without hyperthermia, cells and nanoparticles.**

hyperthermia, can be considered a promising method for the treatment of this cancer. The diameter of the magnetic nanoparticles by TEM, was 8.08 ± 2.5 nm confirming a superparamagnetic property accordance with other studies. The size among the literatures to possess this behavior is different. Some reports noted 7 nm as a critical value,[28] other group limits the diameter between 2–15 nm.[62] As a whole, if the size is less than 20 nm, it could be expected superparamagnetic result.[63] In contrast, accordance with VSM assessment containing coercivity near to 0 Oe, the nanoparticles indicated soft-ferromagnetic considerably. This property implicates excellent heating applications would be observed.[64] Also, no hysteresis and the remanent magnetization as 5 emu/g, are another marks confirming its soft magnetic property.[65] On the other hand, the chemical factor was encapsulated by chitosan and used to inhibit the expression of hsps such as 70 and 90. The size of this compound formulated by chitosan, was 42.42 ± 13.26 nm and 279.04 nm by SEM and DLS, respectively. It is clear this significant variation between the diameters is related to different strategies of both techniques. The DLS method assumes a hydrodynamic value of particle radius relating the average of the diameters from different faces. Usually, the corresponding diameter is larger than the value resulted from SEM. The particles which are visualized by SEM, are not hydrated and free of double layer around the particle.[66] Regarding the formulation of quercetin by chitosan, a previous study reported the size of the particles was 76.58 nm by atomic force microscopy (AFM).[67] Another group obtained 461-482 nm for the quercetin loaded chitosan.[68] This result could be related to different molecular weights of chitosan. In the present study against the noted research groups, the length of chitosan chains was short. Therefore, it was expected that the size of the nanoparticles may be smaller and this observation is in consistent with another research that illustrated smaller particles are developed by using the chitosan with a lower molecular weight.[69] By considering FTIR, both chitosan and quercetin were determined within the whole particle approving successful fabrication of the nanoparticles. Due to abundant primary amine functional groups in the chemical network of chitosan, the prepared chitosan-quercetin nanoparticles act as pH responsive agents.[70] By considering the acidic extracellular pH of tumor tissues due to their poor oxygenation as a function of heterogeneous angiogenesis,[71] this particle may deliver its load when stimulate by lower pH values such as 5.[72] Regarding the cell culture methods, the IC50 concentrations of both nanoparticles were obtained as 10 mg/ml and 0.6 mg/ml, respectively for the magnetic nanomaterial and nanoquercetin. In a similar study by using graphene oxide/cobalt ferrite nanoparticles, the IC50 point is 0.001 g/ml.[25] There is a considerable difference between the studies that could be related to the lower toxicity of free magnetic nanoparticles without graphene oxide. A group reported 54.18 µg/ml as a IC50 value for the corresponding particle[73] that is very lower in compared to the particle density of the present study. The diversity may be explained by considering the concentration of ferric ions which is impressed by the fabrication method. Moreover, a literature presented IC50 as 12.4 µg/ml against MCF-7 cells when the cobalt ferrite doped by Mn.[74] It is clear this less value was resulted due to the toxic effect of manganese which is absent here. On the other hand, the value of quercetin as a noncapsulated particles was 0.02 mg/ml[24] that is significantly lower than the concentration of the nanoformulated particles. This variation may be described because of its lower toxicity after the packing in nanoparticles. A group fabricated nanoquercetin by using low molecular chitosan and the IC50 and diameter of the particles were 10.36 µg/ml and 156.3 nm, respectively.[75] Not only, the size of the nanoparticles was higher, but the concentration for killing at least 50% of cells, was lower in compared with the observations of this study. It could be noted that by increasing the diameter, the toxic effects may be increased. The reason could be discussed accordance with a faster release rate of larger particles[76] and this further delivery, may leads into higher toxicity. For the hyperthermia experiments including DPPH and Real-Time PCR, the frequency and treatment duration were considered accordance with the previous published study as 350 kHz and 10 min, respectively. In this article, these parameters were optimized to increase the temperature to 43°C by using graphene oxide/cobalt ferrite nanoparticles.[25] The therapeutic temperature of this method was in the range of 43–45°C to increase blood circulation to tumor tissue.[77] For DPPH experiment, the OD of the sample groups was converted to radical inhibition (%) accordance with the noted formula in the methods.[78] Thus, a group with higher value (%), contains a more radical amount and accordingly, the possibility of apoptosis is higher. The larger percentages were belonged to the groups which were exposed by hyperthermia and these groups contained both nanoparticle types. In this manner, the groups with the free and encapsulated quercetin showed almost same values. However, the simultaneous treatment indicated a highest value (21.03 ± 0.2 %) in contrast to the less value of the group with only nanocobalt ferrite nanoparticles (8.40 ± 0.15 %). This low level approves weaker apoptosis through radicals due to the absence of quercetin to stop the hsps. As a whole, the group with both nanoparticle types reveals enhanced cell killing in compared to the samples with either quercetin or cobalt ferrite nanoparticles. Concurrently, a study in 2014 by Kumar et al., showed the combination of the Fe_3O_4 nanoparticles and quercetin established stronger cell death in compared to free quercetin in the absence of hyperthermia.[19] The gene expression was another evaluation to advise the impact of the combination treatment under hyperthermia on cell fate. For Bax and Bcl2 genes, it is recommended to compare the ratio of Bax to Bcl2 and the higher value determines lower anticancer resistance.[79] Here, the group with both nanoparticle and hyperthermia condition, depicted the ratio of 6.66 as a highest magnitude. In contrast, the condition with only the nanomagnetic material in the exposure of hyperthermia possessed a less amount. This observation confirms that the high temperature strategy must be collaborated with appropriate anticancer agents. Otherwise, the method is not capable to apply therapeutic response. Regarding the expression of caspase 3 and 8, it should be noted the higher fold change values lead into notable apoptotic incidences. Among the groups, the treatment of nanoquercetin one resulted the highest value of caspase 8 (fold change = 43) and then, the quercetin+cobalt ferrite nanoparticle in combination of hyperthermia is ordered (fold change = 25). In spite of this, the former sample (only NQ) resulted a lower caspase 3 expression (fold change = 0.25) in contrast to the level of the latter group (NQ+Cofe+HT, fold change = 1.4). It seems that caspase 3 was not expressed with any groups except the combination one. By considering the expression of hsps including 70 and 90, the group of NQ with hyperthermia, showed a

lowest amount against the group with only nanoquercetin confirming the significant impact of this nanoparticle on the synthesis of hsps. However, it should be noted it is obvious that the quercetin attenuates the expression of these genes in the presence of hyperthermia. Consistently, an examination described that quercetin decreased the expression degree of hsp70 and 90 more when the sample was treated simultaneously by radiofrequency.[80] Particularly, this result could be highlighted by comparing the NQ+HT against NQ. In contrary, another report revealed the expression of hsp70 was lower in the quercetin group than the combination of this agent with hyperthermia. In other words, by simultaneous applying quercetin and hyperthermia, the percentage of apoptotic cells was enhanced.[81] However, the quercetin was not formulated as nanoparticles and therefore, the compound acted freely independently from the polymeric capsule. On the other hand, the high temperature may apply a shock to the chitosan and increases the rate of release. Moreover, the nanoformulated particle of quercetin can cross the cell membrane rather than hydrophobic agents (free quercetin) and the hsps amount was lower due to the blocking impact of quercetin in NQ group. As a whole, the synergistic strategy of a magnetic material and a chemical component during hyperthermia, leads into a higher value of apoptosis by reducing cell proliferation, radical development and gene expression. However, it is required further investigations particularly in animal models to propose this method eagerly as a new clinical technique.

Conclusion

If the hsps blocker was added to the treated sample by hyperthermia, a more potent apoptosis would be occurred. In this manner, the chaperons are not enough to govern protein folding and therefore, cellular proteins are destroyed by the developed radicals and high temperatures. However, this study is a primitive one that needs more investigations in *in vitro* and *in vivo* models. Nevertheless, the present report could be highlight the importance of signaling pathway modification to result greater cell death in tumor tissues.

Ethics Approval

This study was done under ethical number of IR.SBMU.RETECH.REC.1402.184 from shahid beheshti university of medical sciences, Tehran, Iran.

Consent for Publication

The authors declare consent for publications.

Availability of Data and Materials

All data and materials relevant to this study were included in the results section of this manuscript.

Conflicts of Interest

The authors declare no competing financial and non-financial interests.

Financial Support and Sponsorship

The authors declare no competing financial and non-financial interests.

Author Contributions

Alaa Sameer Neamah: Laboratory experiments
Raziyeh Ghorbani: Laboratory experiments
Mohammad Mahdi Ahadian: Hyperthermia method
Simzar Hosseinzadeh: Grant and supervision
Bahram Kazemi: Supervision

Acknowledgments

The evaluation was carried out by using a grant (ID:43003452) under ethical code of IR.SBMU.RETECH.REC.1402.184 from Medical Nanotechnology and Tissue Engineering Research Center of shahid beheshti university of medical sciences, Tehran, Iran.

References

1. Group EBCTC. Favourable and unfavourable effects on long-term survival of radiotherapy for early breast cancer: an overview of the randomised trials. The Lancet 2000; 355: 1757–70.
2. Raghav PK, Mann Z, Krishnakumar V, Mohanty S. Therapeutic effect of natural compounds in targeting ROS-induced cancer. Handbook of oxidative stress in cancer: Mechanistic aspects: Springer; 2021. p. 1–47.
3. Gopčević KR, Rovčanin BR, Tatić SB, Krivokapić ZV, Gajić MM, Dragutinović VV. Activity of superoxide dismutase, catalase, glutathione peroxidase, and glutathione reductase in different stages of colorectal carcinoma. Digestive diseases and sciences 2013; 58: 2646–52.
4. Lee N, Yoo D, Ling D, Cho MH, Hyeon T, Cheon J. Iron oxide based nanoparticles for multimodal imaging and magnetoresponsive therapy. Chemical reviews 2015; 115: 10637–89.
5. Piñeiro Y, Vargas Z, Rivas J, López-Quintela MA. Iron oxide based nanoparticles for magnetic hyperthermia strategies in biological applications. European Journal of Inorganic Chemistry 2015; 2015: 4495–509.
6. Mameli V. Colloidal $CoFe_2O_4$-based nanoparticles for Magnetic Fluid Hyperthermia. 2016.
7. Takahashi I, Emi Y, Hasuda S, Kakeji Y, Maehara Y, Sugimachi K. Clinical application of hyperthermia combined with anticancer drugs for the treatment of solid tumors. Surgery 2002; 131: S78–S84.
8. Beik J, Abed Z, Ghoreishi FS, Hosseini-Nami S, Mehrzadi S, Shakeri-Zadeh A, et al. Nanotechnology in hyperthermia cancer therapy: From fundamental principles to advanced applications. Journal of Controlled Release 2016; 235: 205–21.
9. Horowitz M, Robinson SD. Heat shock proteins and the heat shock response during hyperthermia and its modulation by altered physiological conditions. Progress in brain research 2007; 162: 433–46.
10. Alberti G, Vergilio G, Paladino L, Barone R, Cappello F, Conway de Macario E, et al. The chaperone system in breast cancer: Roles and therapeutic prospects of the molecular chaperones Hsp27, Hsp60, Hsp70, and Hsp90. International Journal of Molecular Sciences 2022; 23: 7792.
11. Viana P, Hamar P. Targeting the heat shock response induced by modulated electro-hyperthermia (mEHT) in cancer. Biochimica et Biophysica Acta (BBA)-Reviews on Cancer 2024; 189069.
12. Alidadi H, Khorsandi L, Shirani M. Effects of quercetin on tubular cell apoptosis and kidney damage in rats induced by titanium dioxide nanoparticles. The Malaysian Journal of Medical Sciences: MJMS 2018; 25: 72.
13. Cai X, Fang Z, Dou J, Yu A, Zhai G. Bioavailability of quercetin: problems and promises. Current medicinal chemistry 2013; 20: 2572–82.
14. Alizadeh SR, Savadkouhi N, Ebrahimzadeh MA. Drug design strategies that aim to improve the low solubility and poor bioavailability conundrum in quercetin derivatives. Expert Opinion on Drug Discovery 2023; 18: 1117–32.

15. Ernsting MJ, Murakami M, Roy A, Li S-D. Factors controlling the pharmacokinetics, biodistribution and intratumoral penetration of nanoparticles. Journal of controlled release 2013; 172: 782–94.
16. Czepas J, Gwoździński K. The flavonoid quercetin: possible solution for anthracycline-induced cardiotoxicity and multidrug resistance. Biomedicine & pharmacotherapy 2014; 68: 1149–59.
17. Schleich N, Po C, Jacobs D, Ucakar B, Gallez B, Danhier F, et al. Comparison of active, passive and magnetic targeting to tumors of multifunctional paclitaxel/SPIO-loaded nanoparticles for tumor imaging and therapy. Journal of Controlled Release 2014; 194: 82–91.
18. Poornima G, Gupta S, Dhayalan A, Lahiri B, Philip J, Kannan S. Green synthesis of quercetin-loaded magneto-liposomes and their assessment of antioxidant efficacy, hyperthermia and MRI contrast features. Materials Chemistry and Physics 2024; 323: 129663.
19. Kumar SR, Priyatharshni S, Babu V, Mangalaraj D, Viswanathan C, Kannan S, et al. Quercetin conjugated superparamagnetic magnetite nanoparticles for in-vitro analysis of breast cancer cell lines for chemotherapy applications. Journal of colloid and interface science 2014; 436: 234–42.
20. Elbeltagi S, Abdel shakor Ab, M. Alharbi H, Tawfeek HM, Aldosari BN, E. Eldin Z, et al. Synergistic effects of quercetin-loaded $CoFe_2O_4$@ Liposomes regulate DNA damage and apoptosis in MCF-7 cancer cells: based on biophysical magnetic hyperthermia. Drug Development and Industrial Pharmacy 2024; 50: 561–75.
21. Safari M, Naseri M, Esmaeili E, Naderi E. Green synthesis by celery seed extract and improvement of the anticancer activity of quercetin-loaded rGO/Ca1-xMnxFe2O4 nanocarriers using UV light in breast cancer cells. Journal of Molecular Structure 2023; 1281: 135059.
22. Akal Z, Alpsoy L, Baykal A. Superparamagnetic iron oxide conjugated with folic acid and carboxylated quercetin for chemotherapy applications. Ceramics International 2016; 42: 9065–72.
23. Alshehri MA, Panneerselvam C. Development of quercetin loaded biosynthesized chitosan grafted iron oxide nanoformulation and their antioxidant, antibacterial, and anti-cancer properties. Journal of Drug Delivery Science and Technology 2024; 101: 106247.
24. Mobaraki F, Nazari H, Lajevardiyan SA, Hatamie S, Jafary H, Hosseinzadeh S. Synergistic effect of quercetin and cobalt ferrite-graphene oxide-based hyperthermia to inhibit expression of heat shock proteins and induce apoptosis in breast cancer cells. Pharmaceutical Sciences 2022; 28: 552–63.
25. Hatamie S, Balasi ZM, Ahadian MM, Mortezazadeh T, Shams F, Hosseinzadeh S. Hyperthermia of breast cancer tumor using graphene oxide-cobalt ferrite magnetic nanoparticles in mice. Journal of Drug Delivery Science and Technology 2021; 65: 102680.
26. Chandekar KV, Mohan Kant K. Synthesis and characterization of low temperature superparamagnetic cobalt ferrite nanoparticles. Adv Mater Lett 2017; 8: 435–43.
27. El-Okr M, Salem M, Salim M, El-Okr R, Ashoush M, Talaat H. Synthesis of cobalt ferrite nano-particles and their magnetic characterization. Journal of Magnetism and Magnetic Materials 2011; 323: 920–6.
28. Karaagac O, Yildiz BB, Köçkar H. The influence of synthesis parameters on one-step synthesized superparamagnetic cobalt ferrite nanoparticles with high saturation magnetization. Journal of Magnetism and Magnetic Materials 2019; 473: 262–7.
29. Spaldin NA, Mathur ND. Magnetic materials: fundamentals and device applications. Physics Today 2003; 56: 62–3.
30. Jackson M, Solheid P. On the quantitative analysis and evaluation of magnetic hysteresis data. Geochemistry, Geophysics, Geosystems 2010; 11.
31. Ju H, Nam Y, Lee J, Shin H. Anomalous magnetic properties and magnetic phase diagram of La1− xBaxMnO3. Journal of magnetism and magnetic materials 2000; 219: 1–8.
32. Renuka Balakrishna A, James RD. Design of soft magnetic materials. npj Computational Materials 2022; 8: 4.
33. Duraisamy K, Devaraj M, Gangadharan A, Martirosyan KS, Sahu NK, Manogaran P, et al. Single domain soft ferromagnetic ferrofluid suitable for intratumoural magnetic hyperthermia. Colloids and Surfaces A: Physicochemical and Engineering Aspects 2024; 684: 133049.
34. Tran P, Lee S-E, Kim D-H, Pyo Y-C, Park J-S. Recent advances of nanotechnology for the delivery of anticancer drugs for breast cancer treatment. Journal of Pharmaceutical Investigation 2020; 50: 261–70.
35. Niazvand F, Orazizadeh M, Khorsandi L, Abbaspour M, Mansouri E, Khodadadi A. Effects of quercetin-loaded nanoparticles on MCF-7 human breast cancer cells. Medicina 2019; 55: 114.
36. Sadhukhan P, Kundu M, Chatterjee S, Ghosh N, Manna P, Das J, et al. Targeted delivery of quercetin via pH-responsive zinc oxide nanoparticles for breast cancer therapy. Materials science and engineering: C 2019; 100: 129–40.
37. Elsayed AM, Sherif NM, Hassan NS, Althobaiti F, Hanafy NA, Sahyon HA. Novel quercetin encapsulated chitosan functionalized copper oxide nanoparticles as anti-breast cancer agent via regulating p53 in rat model. International Journal of Biological Macromolecules 2021; 185: 134–52.
38. Sun Q. The Raman OH stretching bands of liquid water. Vibrational Spectroscopy 2009; 51: 213–7.
39. Zojaji I, Esfandiarian A, Taheri-Shakib J. Toward molecular characterization of asphaltene from different origins under different conditions by means of FT-IR spectroscopy. Advances in Colloid and Interface Science 2021; 289: 102314.
40. Wang S, Tang Y, Schobert HH, Guo Yn, Su Y. FTIR and 13C NMR investigation of coal component of late Permian coals from southern China. Energy & Fuels 2011; 25: 5672–7.
41. Fuente E, Menéndez J, Díez M, Suárez D, Montes-Morán M. Infrared spectroscopy of carbon materials: a quantum chemical study of model compounds. The Journal of physical chemistry B 2003; 107: 6350-9.
42. Matute AIR, Cardelle-Cobas A, García-Bermejo AB, Montilla A, Olano A, Corzo N. Synthesis, characterization and functional properties of galactosylated derivatives of chitosan through amide formation. Food Hydrocolloids 2013; 33: 245–55.
43. Smith B. The infrared spectra of polymers, VI: Polymers with CO bonds. 2022.
44. Danaei M, Dehghankhold M, Ataei S, Hasanzadeh Davarani F, Javanmard R, Dokhani A, et al. Impact of particle size and polydispersity index on the clinical applications of lipidic nanocarrier systems. Pharmaceutics 2018; 10: 57.
45. Win KY, Feng S-S. Effects of particle size and surface coating on cellular uptake of polymeric nanoparticles for oral delivery of anticancer drugs. Biomaterials 2005; 26: 2713–22.
46. Hasanbegloo K, Banihashem S, Dizaji BF, Bybordi S, Farrokh-Eslamlou N, Abadi PG-s, et al. Paclitaxel-loaded liposome-incorporated chitosan (core)/poly (ε-caprolactone)/chitosan (shell) nanofibers for the treatment of breast cancer. International Journal of Biological Macromolecules 2023; 230: 123380.
47. Kousar K, Shafiq S, Sherazi ST, Iqbal F, Shareef U, Kakar S, et al. In silico ADMET profiling of Docetaxel and development of camel milk derived liposomes nanocarriers for sustained release of Docetaxel in triple negative breast cancer. Scientific Reports 2024; 14: 912.
48. Fang X, Cao J, Shen A. Advances in anti-breast cancer drugs and the application of nano-drug delivery systems in breast cancer therapy. Journal of Drug Delivery Science and Technology 2020; 57: 101662.
49. Krishnamachari V, Levine LH, Paré PW. Flavonoid oxidation by the radical generator AIBN: a unified mechanism for quercetin radical scavenging. Journal of Agricultural and Food Chemistry 2002; 50: 4357–63.
50. Yang J, Xie R, Feng L, Liu B, Lv R, Li C, et al. Hyperthermia and controllable free radical coenhanced synergistic therapy in hypoxia enabled by near-infrared-II light irradiation. ACS nano 2019; 13: 13144–60.
51. Hosseinzadeh S, Nazari H, Esmaeili E, Hatamie S. Polyethylene glycol triggers the anti-cancer impact of curcumin nanoparticles in sw-1736 thyroid cancer cells. Journal of Materials Science: Materials in Medicine 2021; 32: 112.
52. Vatani M, Hosseinzadeh S, Sari A, Rahimpour A, Fattahi R. Apoptotic Impact of Heliox Cold Plasma on a Cervical Cell Line Using Gold Nanoparticle-Doped Graphene Oxide Nanosheets. IJ Pharmaceutical Research; 23.
53. Yang X, Zhong DN, Qin H, Wu PR, Wei KL, Chen G, et al. Caspase-3 over-expression is associated with poor overall survival and clinicopathological parameters in breast cancer: a meta-analysis of 3091 cases. Oncotarget 2017; 9: 8629.
54. Barnes J, Dix D, Collins B, Luft C, Allen J. Expression of inducible Hsp70 enhances the proliferation of MCF-7 breast cancer cells and protects against the cytotoxic effects of hyperthermia. Cell stress & chaperones 2001; 6: 316.
55. Cardoso F, Senkus E, Costa A, Papadopoulos E, Aapro M, André F, et al. 4th ESO–ESMO international consensus guidelines for advanced breast cancer (ABC 4). Annals of Oncology 2018; 29: 1634–57.
56. Aalinkeel R, Bindukumar B, Reynolds JL, Sykes DE, Mahajan SD, Chadha KC, et al. The dietary bioflavonoid, quercetin, selectively induces apoptosis of prostate cancer cells by down-regulating the expression of heat shock protein 90. The Prostate 2008; 68: 1773–89.
57. Srivastava NS, Srivastava RAK. Curcumin and quercetin synergistically inhibit cancer cell proliferation in multiple cancer cells and modulate Wnt/β-catenin signaling and apoptotic pathways in A375 cells. Phytomedicine 2019; 52: 117–28.
58. Chen SF, Nieh S, Jao SW, Liu CL, Wu CH, Chang YC, et al. Quercetin suppresses drug-resistant spheres via the p38 MAPK–Hsp27 apoptotic pathway in oral cancer cells. PloS one 2012; 7: e49275.
59. Wang G, Wang JJ, Chen XL, Du L, Li F. Quercetin-loaded freeze-dried nanomicelles: Improving absorption and anti-glioma efficiency in vitro and in vivo. Journal of Controlled Release 2016; 235: 276–90.

60. Jain S, Jain AK, Pohekar M, Thanki K. Novel self-emulsifying formulation of quercetin for improved in vivo antioxidant potential: implications for drug-induced cardiotoxicity and nephrotoxicity. Free Radical Biology and Medicine 2013; 65: 117–30.
61. Hazra M, Mandal DD, Mandal T, Bhuniya S, Ghosh M. Designing polymeric microparticulate drug delivery system for hydrophobic drug quercetin. Saudi pharmaceutical journal 2015; 23: 429–36.
62. Vázquez-Vázquez C, López-Quintela M, Buján-Núñez M, Rivas J. Finite size and surface effects on the magnetic properties of cobalt ferrite nanoparticles. Journal of Nanoparticle Research 2011; 13: 1663-76.
63. Ozkaya T, Toprak MS, Baykal A, Kavas H, Köseoğlu Y, Aktaş B. Synthesis of Fe_3O_4 nanoparticles at 100 C and its magnetic characterization. Journal of Alloys and Compounds 2009; 472: 18–23.
64. Singh R, Alonso J, Devkota J, Phan M-H. Soft Ferromagnetic Microwires with Excellent Inductive Heating Properties for Clinical Hyperthermia Applications. High Performance Soft Magnetic Materials 2017; 151–67.
65. Shi P. One-dimensional magneto-mechanical model for anhysteretic magnetization and magnetostriction in ferromagnetic materials. Journal of Magnetism and Magnetic Materials 2021; 537: 168212.
66. de la Calle I, Soto-Gómez D, Pérez-Rodríguez P, López-Periago JE. Particle size characterization of sepia ink eumelanin biopolymers by SEM, DLS, and AF4-MALLS: a comparative study. Food Analytical Methods 2019; 12: 1140–51.
67. Zhang Y, Yang Y, Tang K, Hu X, Zou G. Physicochemical characterization and antioxidant activity of quercetin-loaded chitosan nanoparticles. Journal of Applied Polymer Science 2008; 107: 891–7.
68. Kim ES, Lee J-S, Lee HG. Quercetin delivery characteristics of chitosan nanoparticles prepared with different molecular weight polyanion cross-linkers. Carbohydrate Polymers 2021; 267: 118157.
69. Villegas-Peralta Y, López-Cervantes J, Madera Santana TJ, Sánchez-Duarte RG, Sánchez-Machado DI, Martínez-Macías MdR, et al. Impact of the molecular weight on the size of chitosan nanoparticles: Characterization and its solid-state application. Polymer Bulletin 2021; 78: 813–32.
70. Popat A, Liu J, Lu GQM, Qiao SZ. A pH-responsive drug delivery system based on chitosan coated mesoporous silica nanoparticles. Journal of Materials Chemistry 2012; 22: 11173–8.
71. Schornack PA, Gillies RJ. Contributions of cell metabolism and H+ diffusion to the acidic pH of tumors. Neoplasia 2003; 5: 135–45.
72. Barar J, Omidi Y. Dysregulated pH in tumor microenvironment checkmates cancer therapy. BioImpacts: BI 2013; 3: 149.
73. Venkataramaiah S, Venkatappa MM, Udagani C, Sannaningaiah D. Green-Synthesized Cobalt Ferrite Nanoparticle Alleviated Sodium Nitrite-Induced Oxidative Stress Through Its Anti-oxidant Property and Displayed Anti-inflammatory, Anti-diabetic and Anti-platelet Activities. Journal of Superconductivity and Novel Magnetism 2024; 1–19.
74. Fiaz S, Ahmed MN, ul Haq I, Shah SWA, Waseem M. Green synthesis of cobalt ferrite and Mn doped cobalt ferrite nanoparticles: Anticancer, antidiabetic and antibacterial studies. Journal of Trace Elements in Medicine and Biology 2023; 80: 127292.
75. Kamyabi R, Jahandideh A, Panahi N, Muhammadnejad S. Synergistic cytotoxicity effect of the combination of chitosan nanoencapsulated imatinib mesylate and quercetin in BCR-ABL positive K562 cells. Iranian Journal of Basic Medical Sciences 2023; 26: 359.
76. Caster JM, Stephanie KY, Patel AN, Newman NJ, Lee ZJ, Warner SB, et al. Effect of particle size on the biodistribution, toxicity, and efficacy of drug-loaded polymeric nanoparticles in chemoradiotherapy. Nanomedicine: Nanotechnology, Biology and Medicine 2017; 13: 1673-83.
77. Emami B, Song CW. Physiological mechanisms in hyperthermia: a review. International Journal of Radiation Oncology* Biology* Physics 1984; 10: 289–95.
78. Siahpoosh A, Alikhani K. Evaluation of antioxidant capacity and free radical scavenging activities of pepsin extract of cuttlefish (Sepia pharaonis) from Persian Gulf. 2016.
79. Raisova M, Hossini AM, Eberle J, Riebeling C, Orfanos CE, Geilen CC, et al. The Bax/Bcl-2 ratio determines the susceptibility of human melanoma cells to CD95/Fas-mediated apoptosis. Journal of investigative dermatology 2001; 117: 333–40.
80. Yang W, Cui M, Lee J, Gong W, Wang S, Fu J, et al. Heat shock protein inhibitor, quercetin, as a novel adjuvant agent to improve radiofrequency ablation-induced tumor destruction and its molecular mechanism. Chinese journal of cancer research 2016; 28: 19.
81. Shen J, Zhang W, Wu J, Zhu Y. The synergistic reversal effect of multidrug resistance by quercetin and hyperthermia in doxorubicin-resistant human myelogenous leukemia cells. International journal of hyperthermia 2008; 24: 151–9.